

Electronic Supplementary Information

Low-cost batteries based on industrial waste Al-Si microparticles and LiFePO₄ for stationary energy storage

Nan Zhang,^a Chuangchao Sun,^a Yiqiang Huang,^a Ling Lv,^a Zunchun Wu,^a Chunnan
Zhu,^a Xuancheng Wang,^a Xuezhong Xiao,^a Xiulin Fan,^{*a} and Lixin Chen^{*a}

^a State Key Laboratory of Silicon Materials, School of Materials Science and
Engineering, Zhejiang University, Hangzhou 310027, China.

* Corresponding author email: xlfan@zju.edu.cn; lxchen@zju.edu.cn

Supplementary Note

1. Discussion of chemical stability of LiPF₆ ether electrolytes

Although ether-based electrolytes showed promising prospects for alloy anodes, not all ethers are adaptable with the most common salt, LiPF₆. Only several ethers with a specific structure exhibit good compatibility with LiPF₆. We studied the physical state changes of various commonly used ethers solvents containing 1.0 M LiPF₆ along with time, including THF, 2-MeTHF, THF/2-MeTHF (THF: 2-MeTHF = 1:1, vol.), dimethoxyethane (DME), 1,3-dioxolane (DOL). At the very beginning of adding 1.0 M LiPF₆ to the mentioned five ether solvents and baseline EC/DMC solvent, colorless (or slightly yellow) and transparent solutions were acquired for all the above solvents. After only 5 minutes, a violent reaction accompanied by heat generation was observed in DOL solvent, and the overall solution transformed to gelatinous soon. The reaction of LiPF₆ with LiPF₆ and DME occurred soon after and lasted for several days. Eventually, the whole solution of THF electrolyte and ~1/3 of DME electrolyte converted to gelatinous. There are no noticeable state changes in 2-MeTHF, THF/2-MeTHF, and EC/DMC solutions after one month.

2. Discussion of chemical stability of LiPF₆ ether electrolytes

We compared the solvation structure information from the Raman band shift of the PF₆⁻ anion in various electrolytes. As Fig. S15 shows, an increased Raman peak blueshift of the ~741 cm⁻¹ band¹ assigned to PF₆⁻ was observed in the sequence of 1.0 M LiPF₆ EC/DMC < 1.0 M LiPF₆ 2-MeTHF < 2.0 M LiPF₆ 2-MeTHF, which suggests the rising ionic association between PF₆⁻ and Li⁺. The strong PF₆⁻···Li⁺ binding energy in 2-MeTHF-based electrolytes leads to the formation of contact ion pairs (CIPs) and aggregates (AGGs).^{2, 3} In addition, the blueshift of CH₂ stretch Raman shift showed a decrease in the following order: 1.0 M LiPF₆ EC/DMC > 2.0 M LiPF₆ 2-MeTHF > 1.0

M LiPF₆ 2-MeTHF, which means the reduced solvation ability in 2-MeTHF-based electrolytes. The combination of these two factors renders an elevated LiPF₆ reduction potential much prior to the ether solvent,⁴ facilitating the formation of LiF and suppressing the decomposition of the solvent. We finally chose to use 2.0 M LiPF₆ 2-MeTHF for the subsequent tests based on the above analysis.

Supplementary Figure

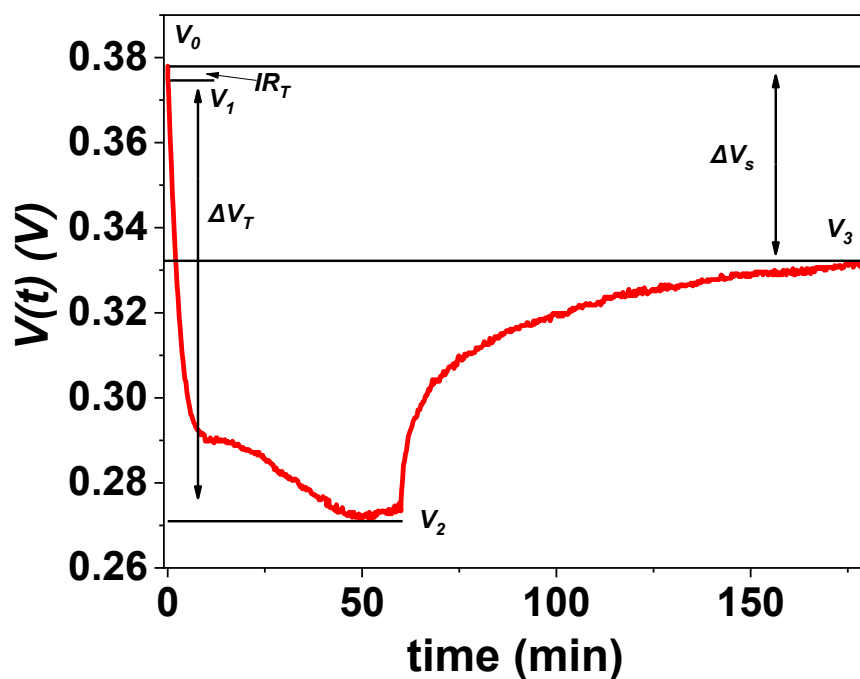


Fig. S1 A typical magnified voltage-time profile of one discharge pulse derived from GITT.

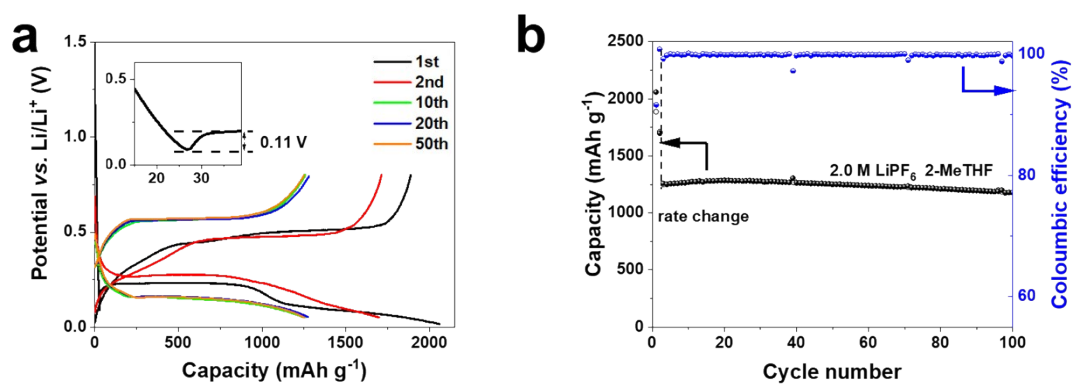


Fig. S2 a) Typical charge/discharge profiles and **b)** Cycling stability and CE of Al-SiMP electrode cycled in 2.0 M LiPF₆ 2-MeTHF. The rates were C/10 at the initial 2 cycles and 2C at the subsequent cycles.

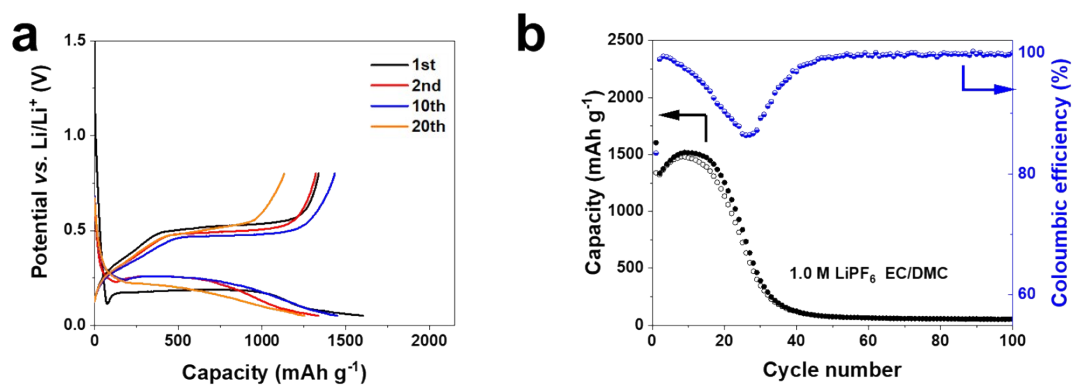


Fig. S3 a) Typical charge/discharge profiles and **b)** Cycling stability and CE of Al-SiMP electrode cycled in 1.0 M LiPF₆ EC/DMC. The rate was C/10.

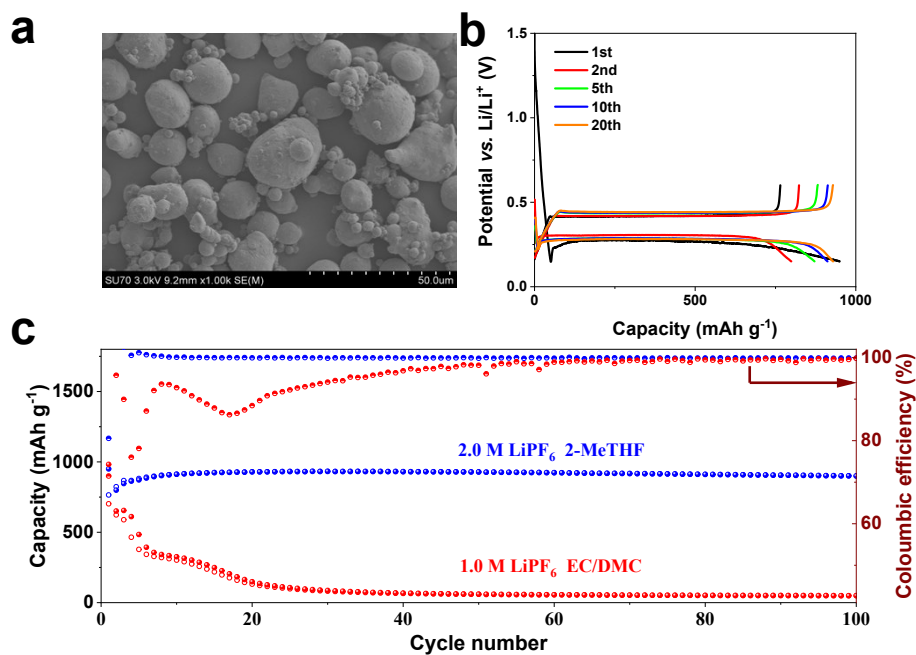


Fig. S4 a) SEM images of AlMPs. **b)** Voltage profiles of AlMPs cycled in 2.0 M LiPF₆ 2-MeTHF electrolyte. **c)** Cycling performance and CEs of AlMPs cycled in 2.0 M LiPF₆ 2-MeTHF electrolyte.

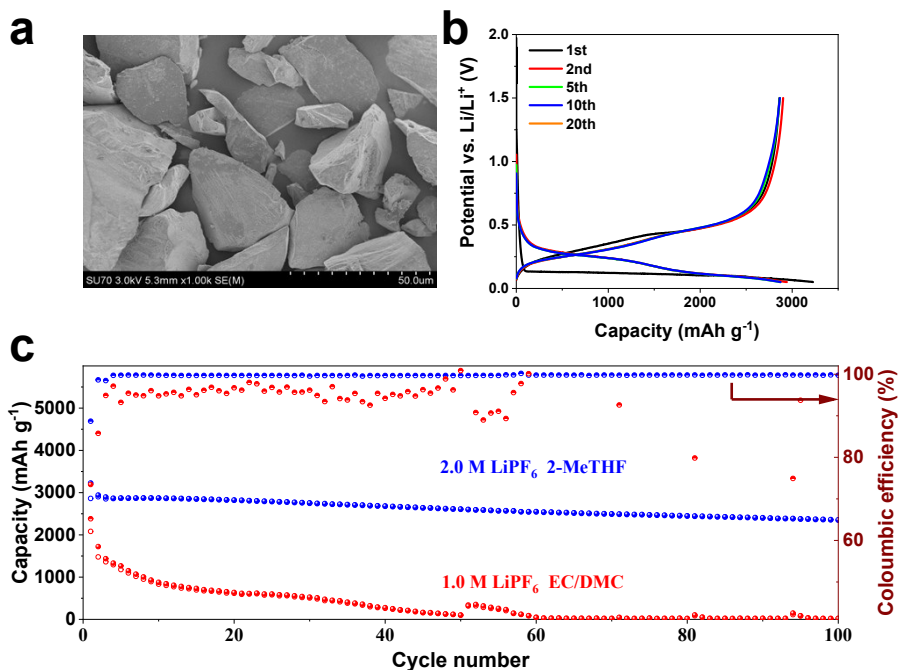


Fig. S5 a) SEM images of SiMPs. b) Voltage profiles of SiMPs cycled in 2.0 M LiPF₆ 2-MeTHF electrolyte. c) Cycling performance and CEs of SiMPs cycled in 2.0 M LiPF₆ 2-MeTHF electrolyte.

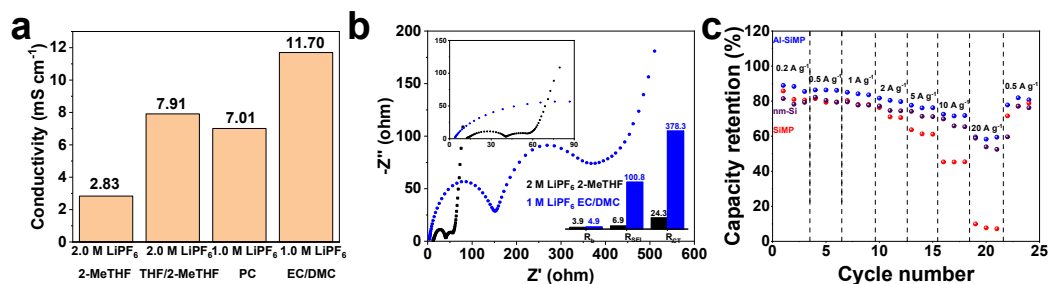


Fig. S6 a) Ionic conductivity comparison of various electrolytes. b) EIS in Nyquist plots of Al-SiMPs in 2.0 M LiPF₆ 2-MeTHF electrolyte (black), 1.0 M LiPF₆/EC-DMC electrolyte (blue). c) The comparison of rate performance of Al-SiMP (blue), nano-Si (purple), and SiMP (red).

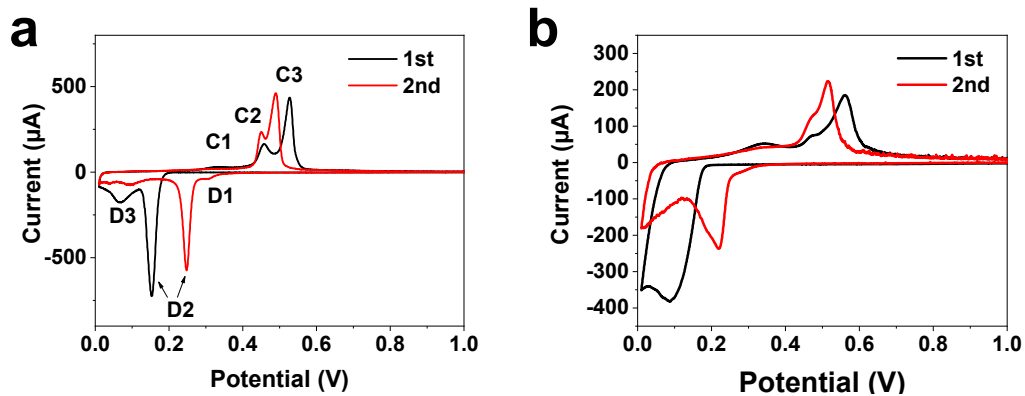


Fig. S7 CV curves of Al-SiMPs cycled in **a)** 2.0 M LiPF_6 2-MeTHF and **b)** 1.0 M $\text{LiPF}_6/\text{EC-DMC}$ electrolyte.

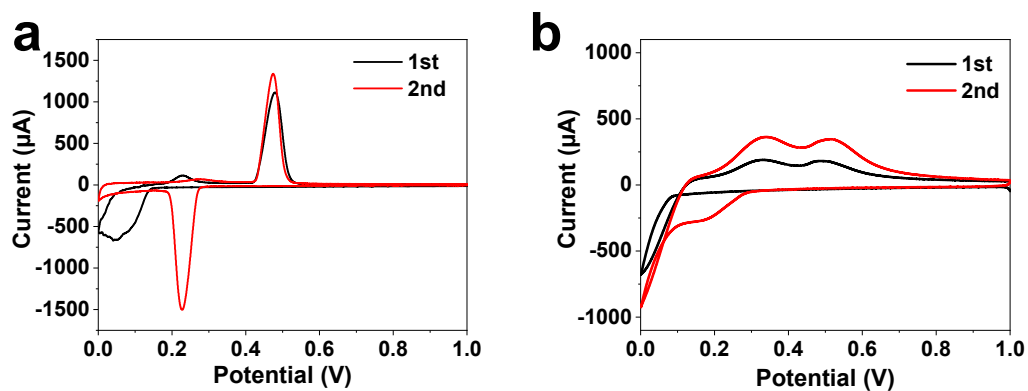


Fig. S8 CV curves of **a)** AlMPs, **b)** SiMPs cycled in 2.0 M LiPF_6 2-MeTHF.

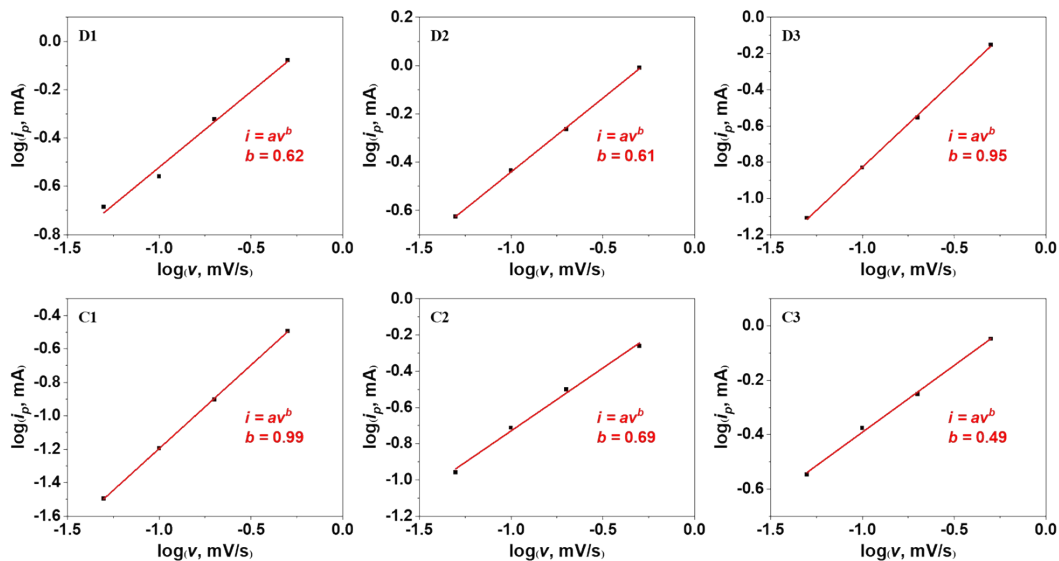


Fig. S9 Log i (peak current) vs. log v (scan rate) plots at charging/discharging from the CV curves of Al-SiMPs.

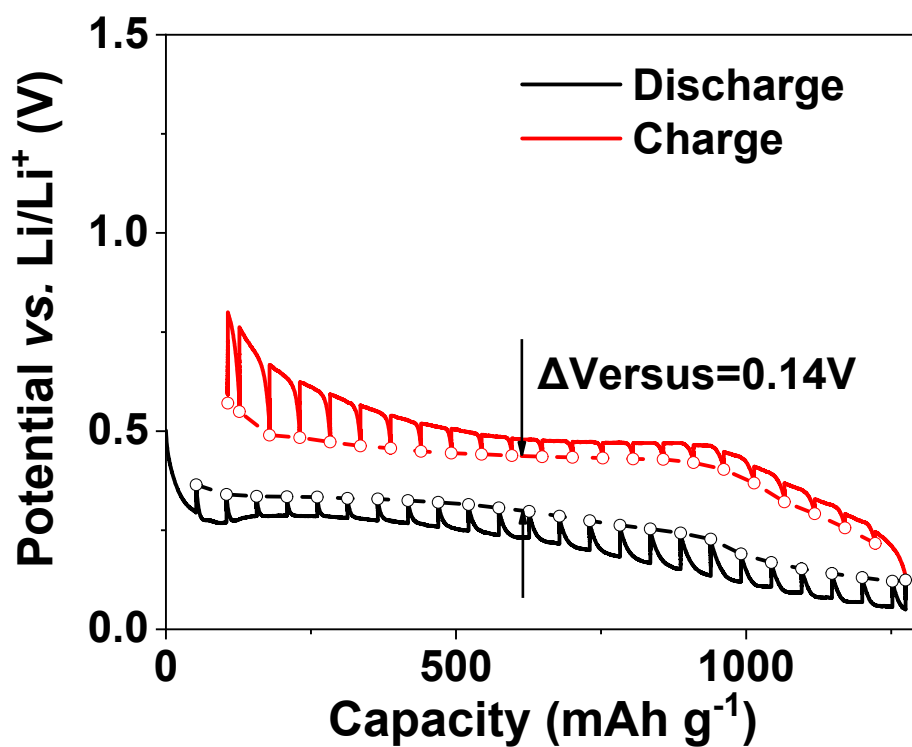


Fig. S10 GITT profiles of Al-SiMPs in 1.0 M LiPF₆ EC/DMC.

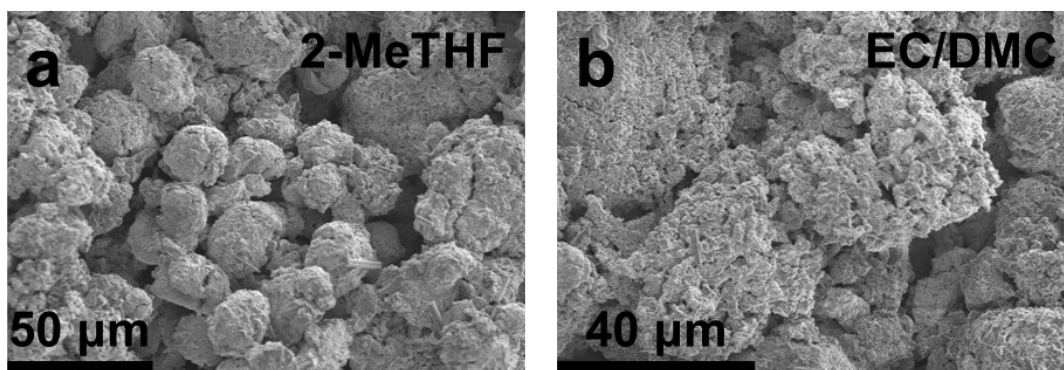


Fig. S11 SEM images of **a)** Al-SiMPs cycled in 2.0 M LiPF₆ 2-MeTHF electrolyte after 5 cycles, and **b)** Al-SiMPs cycled in 1.0 M LiPF₆ EC/DMC electrolyte after 5 cycles.

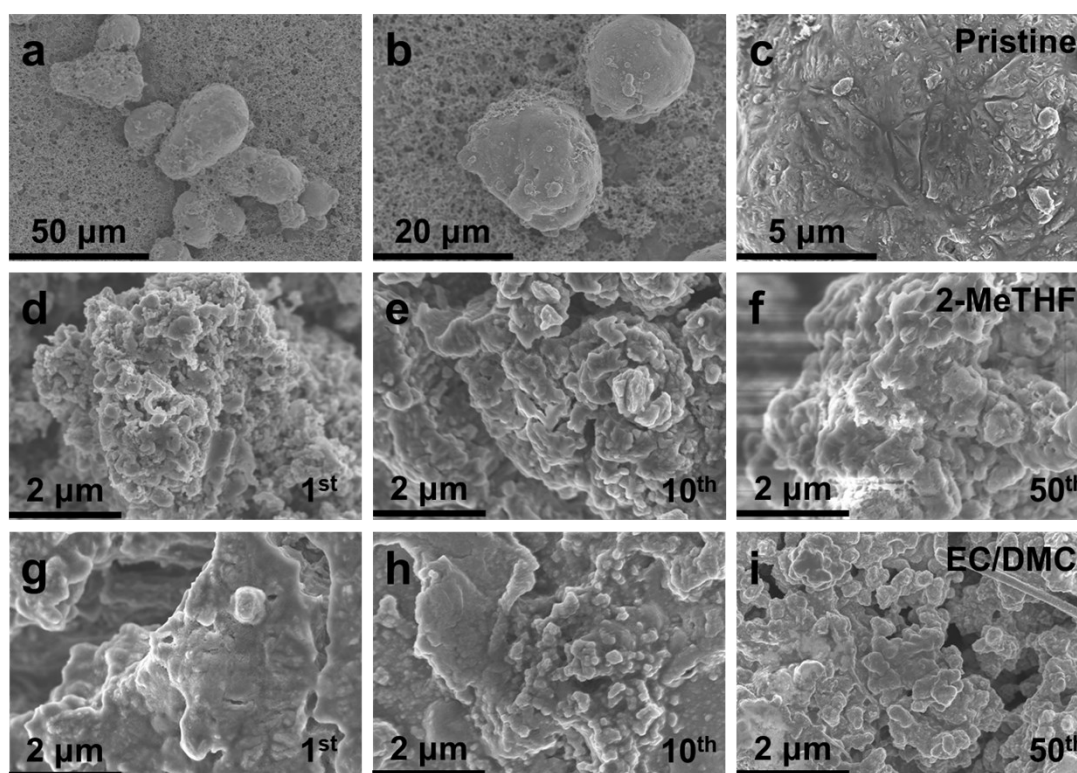


Fig. S12 SEM images of **a), b) c)** pristine Al-SiMPs. **d), e), f)** Al-SiMPs cycled in 2.0 M LiPF₆ 2-MeTHF electrolyte after 1, 10, 50 cycles. **g), h), i)** Al-SiMPs cycled in 1.0 M LiPF₆/EC-DMC electrolyte after 1, 10, 50 cycles.

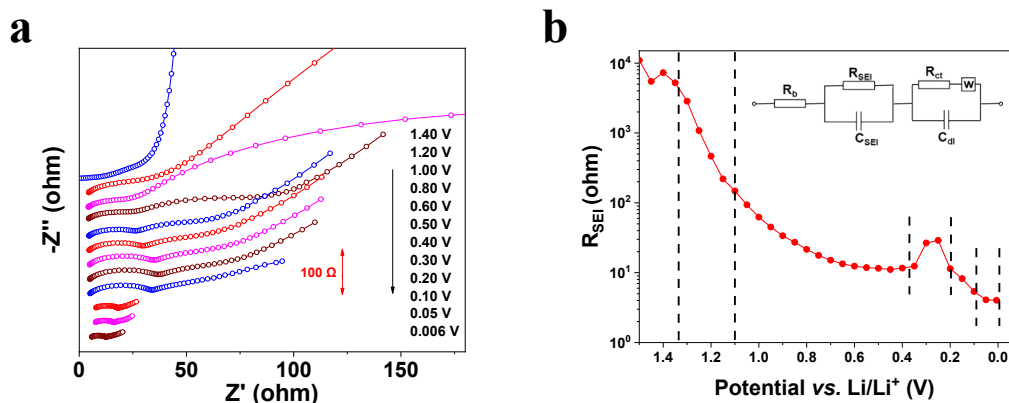


Fig. S13 a) EIS of Al-Si electrode in the 2-MeTHF-based electrolyte at various potentials recorded during the first lithiation process: from 1.4 V to 0.006 V. **b)** Potential dependences of R_{SEI} of the Al-Si anode in the 2-MeTHF-based electrolyte.

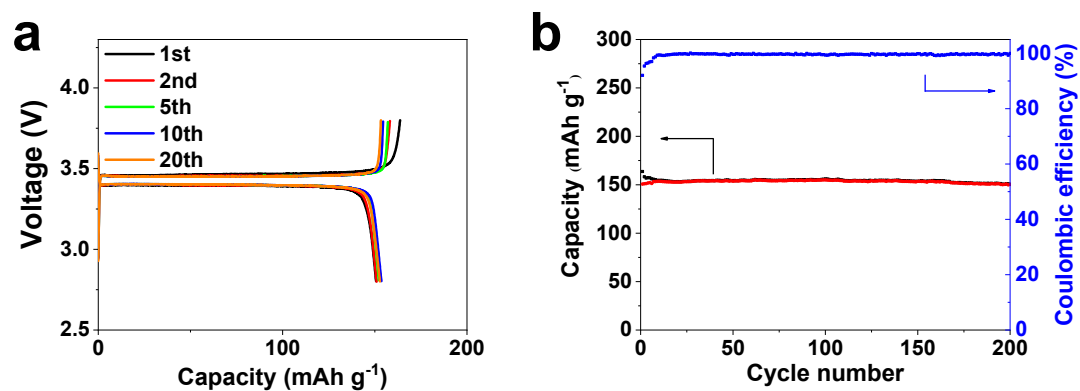


Fig. S14 a) Voltage profiles and **b)** cycling performance of LFP cathode cycled in 2.0 M LiPF_6 2-MeTHF electrolyte.

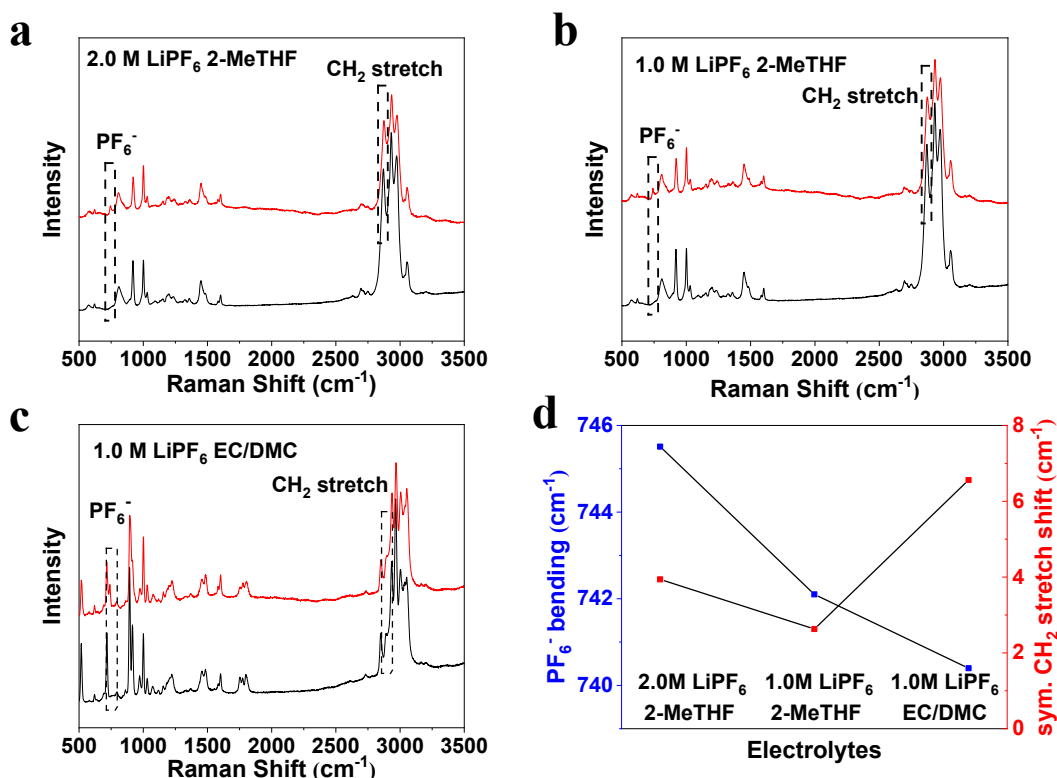


Fig. S15 Raman spectra of various electrolytes with their pure solvent: a) 2.0 M LiPF₆ 2-MeTHF, b) 1.0 M LiPF₆ 2-MeTHF, c) 1.0 M LiPF₆ EC/DMC. d) The peak shift trend of PF₆⁻ and CH₂ stretch.

Reference

- [1] C.M. Burba, R. Frech, *J. Phys. Chem. B*, 2005, **109**, 15161-15164.
- [2] J. Ming, Z. Cao, W. Wahyudi, M.L. Li, P. Kumar, Y.Q. Wu, J.Y. Hwang, M.N. Hedhili, L. Cavallo, Y.K. Sun, L.J. Li, *Acs Energy Lett.* 2018, **3**, 335-340.
- [3] Y. Yamada, K. Furukawa, K. Sodeyama, K. Kikuchi, M. Yaegashi, Y. Tateyama, A. Yamada, *J. Am. Chem. Soc.* 2014, **136**, 5039-46.
- [4] J. Chen, X. Fan, Q. Li, H. Yang, M.R. Khoshi, Y. Xu, S. Hwang, L. Chen, X. Ji, C. Yang, H. He, C. Wang, E. Garfunkel, D. Su, O. Borodin, C. Wang, *Nat. Energy* 2020, **5**, 386-397.